Operation Highlights in 2023 – 2025

Machine Availability

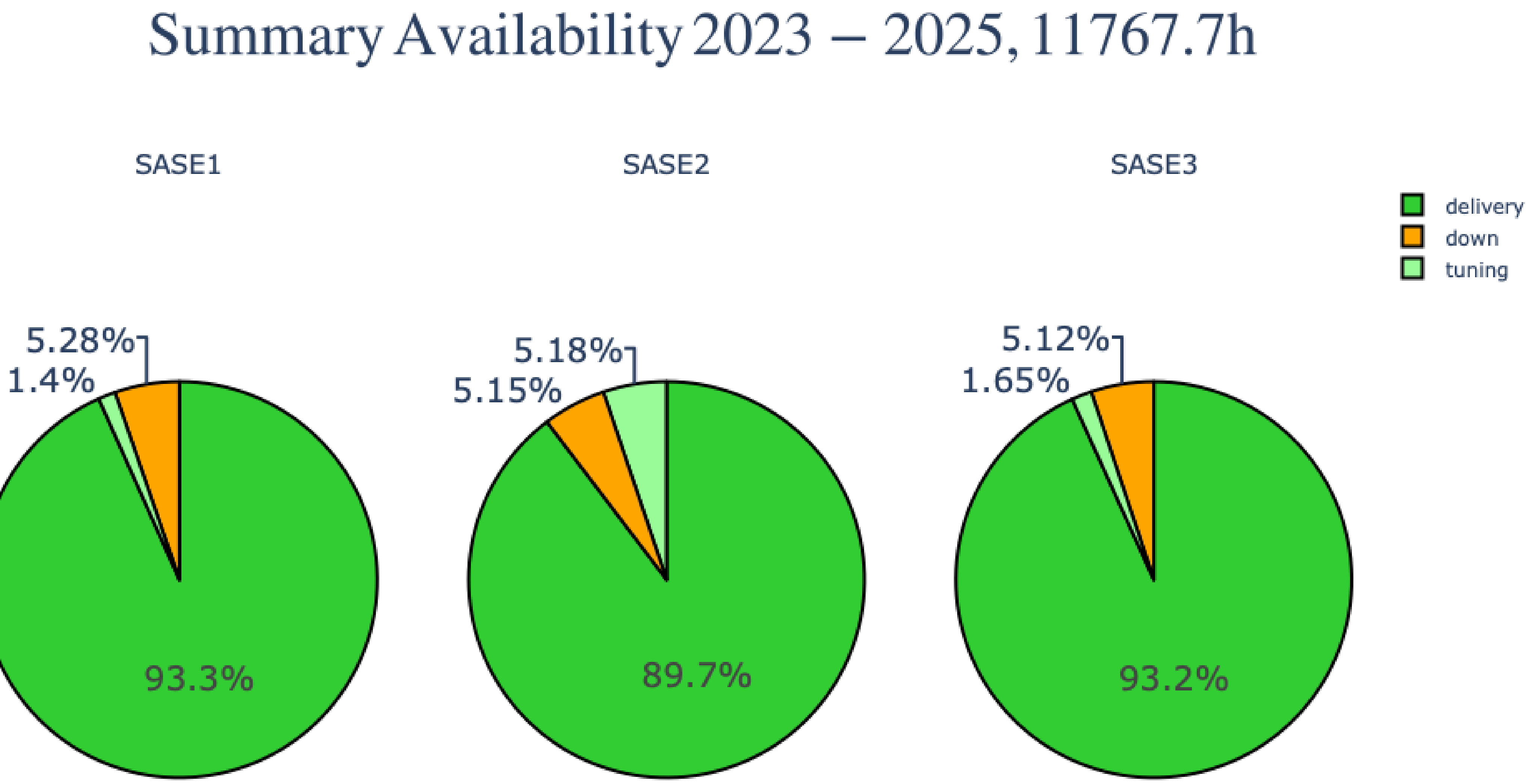

2023

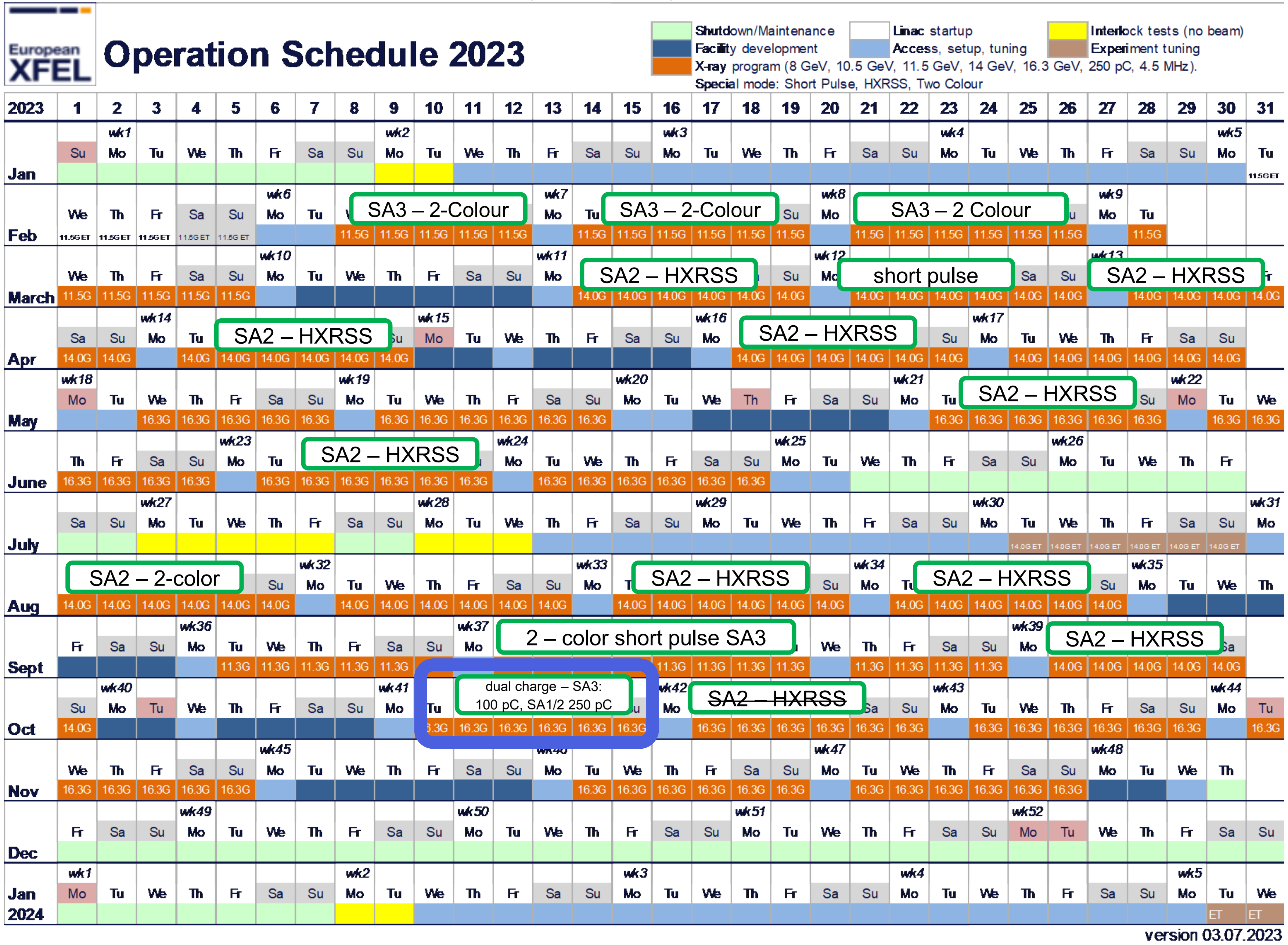
European XFEL
Operation Schedule 2023
Shutdown/Maintenance
Facility development
X-ray program (8 GeV, 10.5 GeV, 11.5 GeV, 14 GeV, 16.3 GeV, 250 pC, 4.5 MHz).
Special mode: Short Pulse, HXRSS, Two Colour
Linac startup
Access, setup, tuning
Interlock tests (no beam)
Experiment tuning
SA3 – 2-Colour
SA3 – 2-Colour
SA3 – 2 Colour
SA2 – HXRSS
short pulse
SA2 – HXRSS
SA2 – HXRSS
SA2 – HXRSS
SA2 – HXRSS
SA2 – HXRSS
SA2 – 2-color
SA2 – HXRSS
SA2 – HXRSS
2 – color short pulse SA3
SA2 – HXRSS
dual charge – SA3: 100 pC, SA1/2 250 pC
SA2 – HXRSS
version 03.07.2023

Dual Charge, excellent performance – cw 41

- 16.2 GeV, 250 pC, non interleaved mode, 150pC in beam region 3 (SASE3)
- SASE1: 4.5mJ @ 9.3 keV / up to 5 mJ @ 7.8keV FXE (user #4237 - Sacchi)
- SASE2: 650-700 uJ @ 18.8 keV HED (user #4520 - Tracy)
- SASE3: 400 uJ @ 1 keV, short pulses (sub fs) SQS (IHR)

FXE

Ultrafast structural dynamics driven by laser-induced demagnetization in presence of strong spin-phonon coupling

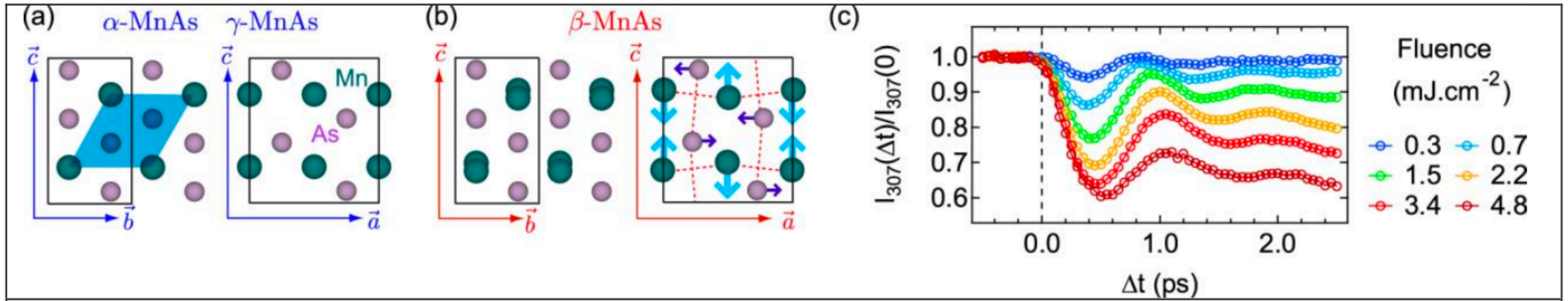

Figure 1. Crystallographic structure of hexagonal **α**- and γ-MnAs (a) and of orthorhombic **β**-MnAs (b), using the conventional orthorhombic cell notation for all phases. (c) Transient evolution of the **β**-MnAs **307** reflection following an optical excitation (from ref. [vid]).

HED

Phase transitions in amorphous materials under shock compression

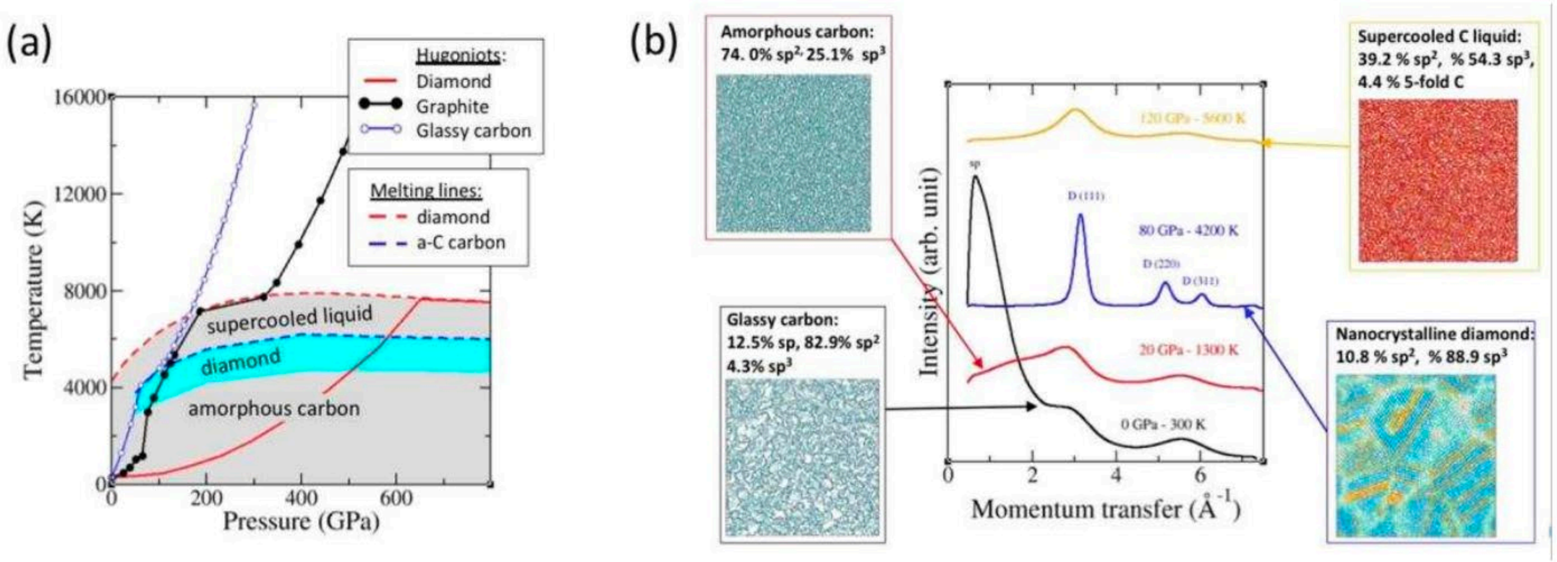

2023

European XFEL

Operation Schedule 2023

Shutdown/Maintenance | Linac startup | Interlock tests (no beam) | Facility development | Access, setup, tuning | Experiment tuning | X-ray program (8 GeV, 10.5 GeV, 11.5 GeV, 14 GeV, 16.3 GeV, 250 pC, 4.5 MHz). | Special mode: Short Pulse, HXRSS, Two Colour

2023	1	2	3	4	5	6	7	8	9	10	11	12	13	14	15	16	17	18	19	20	21	22	23	24	25	26	27	28	29	30	31
Jan	Su	wk1 Mo	Tu	We	Th	Fr	Sa	Su	wk2 Mo	Tu	We	Th	Fr	Sa	Su	wk3 Mo	Tu	We	Th	Fr	Sa	Su	wk4 Mo	Tu	We	Th	Fr	Sa	Su	wk5 Mo	Tu 11.5G ET
Feb	We 11.5G ET	Th 11.5G ET	Fr 11.5G ET	Sa 11.5G ET	Su 11.5G ET	wk6 Mo	Tu	We 11.5G	Th 11.5G	Fr 11.5G	Sa 11.5G	Su 11.5G	wk7 Mo	Tu 11.5G	We 11.5G	Th 11.5G	Fr 11.5G	Sa 11.5G	Su 11.5G	wk8 Mo	Tu 11.5G	We 11.5G	Th 11.5G	Fr 11.5G	Sa 11.5G	Su 11.5G	wk9 Mo	Tu 11.5G			
March	We 11.5G	Th 11.5G	Fr 11.5G	Sa 11.5G	Su 11.5G	wk10 Mo	Tu	We	Th	Fr	Sa	Su	wk11 Mo	Tu 14.0G	We 14.0G	Th 14.0G	Fr 14.0G	Sa 14.0G	Su 14.0G	wk12 Mo	Tu 14.0G	We 14.0G	Th 14.0G	Fr 14.0G	Sa 14.0G	Su 14.0G	wk13 Mo	Tu 14.0G	We 14.0G	Th 14.0G	Fr 14.0G
Apr	Sa 14.0G	Su 14.0G	wk14 Mo	Tu 14.0G	We 14.0G	Th 14.0G	Fr 14.0G	Sa 14.0G	Su 14.0G	wk15 Mo	Tu	We	Th	Fr	Sa	Su	wk16 Mo	Tu 14.0G	We 14.0G	Th 14.0G	Fr 14.0G	Sa 14.0G	Su 14.0G	wk17 Mo	Tu 14.0G	We 14.0G	Th 14.0G	Fr 14.0G	Sa 14.0G	Su 14.0G	
May	wk18 Mo	Tu	We 16.3G	Th 16.3G	Fr 16.3G	Sa 16.3G	Su 16.3G	wk19 Mo	Tu 16.3G	We 16.3G	Th 16.3G	Fr 16.3G	Sa 16.3G	Su 16.3G	wk20 Mo	Tu	We	Th	Fr	Sa	Su	wk21 Mo	Tu 16.3G	We 16.3G	Th 16.3G	Fr 16.3G	Sa 16.3G	Su 16.3G	wk22 Mo	Tu 16.3G	We 16.3G
June	Th 16.3G	Fr 16.3G	Sa 16.3G	Su 16.3G	wk23 Mo	Tu 16.3G	We 16.3G	Th 16.3G	Fr 16.3G	Sa 16.3G	Su 16.3G	wk24 Mo	Tu 16.3G	We 16.3G	Th 16.3G	Fr 16.3G	Sa 16.3G	Su 16.3G	wk25 Mo	Tu	We	Th	Fr	Sa	Su	wk26 Mo	Tu	We	Th	Fr	
July	Sa	Su	wk27 Mo	Tu	We	Th	Fr	Sa	Su	wk28 Mo	Tu	We	Th	Fr	Sa	Su	wk29 Mo	Tu	We	Th	Fr	Sa	Su	wk30 Mo	Tu 14.0G ET	We 14.0G ET	Th 14.0G ET	Fr 14.0G ET	Sa 14.0G ET	Su 14.0G ET	wk31 Mo
Aug	Tu 14.0G	We 14.0G	Th 14.0G	Fr 14.0G	Sa 14.0G	Su 14.0G	wk32 Mo	Tu 14.0G	We 14.0G	Th 14.0G	Fr 14.0G	Sa 14.0G	Su 14.0G	wk33 Mo	Tu 14.0G	We 14.0G	Th 14.0G	Fr 14.0G	Sa 14.0G	Su 14.0G	wk34 Mo	Tu 14.0G	We 14.0G	Th 14.0G	Fr 14.0G	Sa 14.0G	Su 14.0G	wk35 Mo	Tu	We	Th
Sept	Fr	Sa	Su	wk36 Mo	Tu 11.3G	We 11.3G	Th 11.3G	Fr 11.3G	Sa 11.3G	Su 11.3G	wk37 Mo	Tu 11.3G	We 11.3G	Th 11.3G	Fr 11.3G	Sa 11.3G	Su 11.3G	Mo 11.3G	Tu 11.3G	We	Th 11.3G	Fr 11.3G	Sa 11.3G	Su 11.3G	wk39 Mo	Tu 14.0G	We 14.0G	Th 14.0G	Fr 14.0G	Sa 14.0G	
Oct	Su	wk40 Mo	Tu	We	Th	Fr	Sa	Su	wk41 Mo	Tu 16.3G	We 16.3G	Th 16.3G	Fr 16.3G	Sa 16.3G	Su 16.3G	wk42 Mo	Tu 16.3G	We 16.3G	Th 16.3G	Fr 16.3G	Sa 16.3G	Su 16.3G	wk43 Mo	Tu 16.3G	We 16.3G	Th 16.3G	Fr 16.3G	Sa 16.3G	Su 16.3G	wk44 Mo	Tu 16.3G
Nov	We 16.3G	Th 16.3G	Fr 16.3G	Sa 16.3G	Su 16.3G	wk45 Mo	Tu	We	Th	Fr	Sa	Su	wk46 Mo	Tu 16.3G	We 16.3G	Th 16.3G	Fr 16.3G	Sa 16.3G	Su 16.3G	wk47 Mo	Tu 16.3G	We 16.3G	Th 16.3G	Fr 16.3G	Sa 16.3G	Su 16.3G	wk48 Mo	Tu	We	Th	
Dec	Fr	Sa	Su	wk49 Mo	Tu	We	Th	Fr	Sa	Su	wk50 Mo	Tu	We	Th	Fr	Sa	Su	wk51 Mo	Tu	We	Th	Fr	Sa	Su	wk52 Mo	Tu	We	Th	Fr	Sa	Su
Jan 2024	wk1 Mo	Tu	We	Th	Fr	Sa	Su	wk2 Mo	Tu	We	Th	Fr	Sa	Su	wk3 Mo	Tu	We	Th	Fr	Sa	Su	wk4 Mo	Tu	We	Th	Fr	Sa	Su	wk5 Mo	Tu ET	We ET

SA3 – 2-Colour

SA3 – 2-Colour

SA3 – 2 Colour

SA2 – HXRSS

short pulse

SA2 – HXRSS

SA2 – HXRSS

SA2 – HXRSS

SA2 – HXRSS

SA2 – HXRSS

SA2 – 2-color

SA2 – HXRSS

SA2 – HXRSS

2 – color short pulse SA3

SA2 – HXRSS

dual charge – SA3: 100 pC, SA1/2 250 pC

SA2 – HXRSS

version 03.07.2023

- High pulse energy performance (~800 – 900 uJ) at 19 keV @ SA1 in cw 44 during normal X-Ray Delivery week

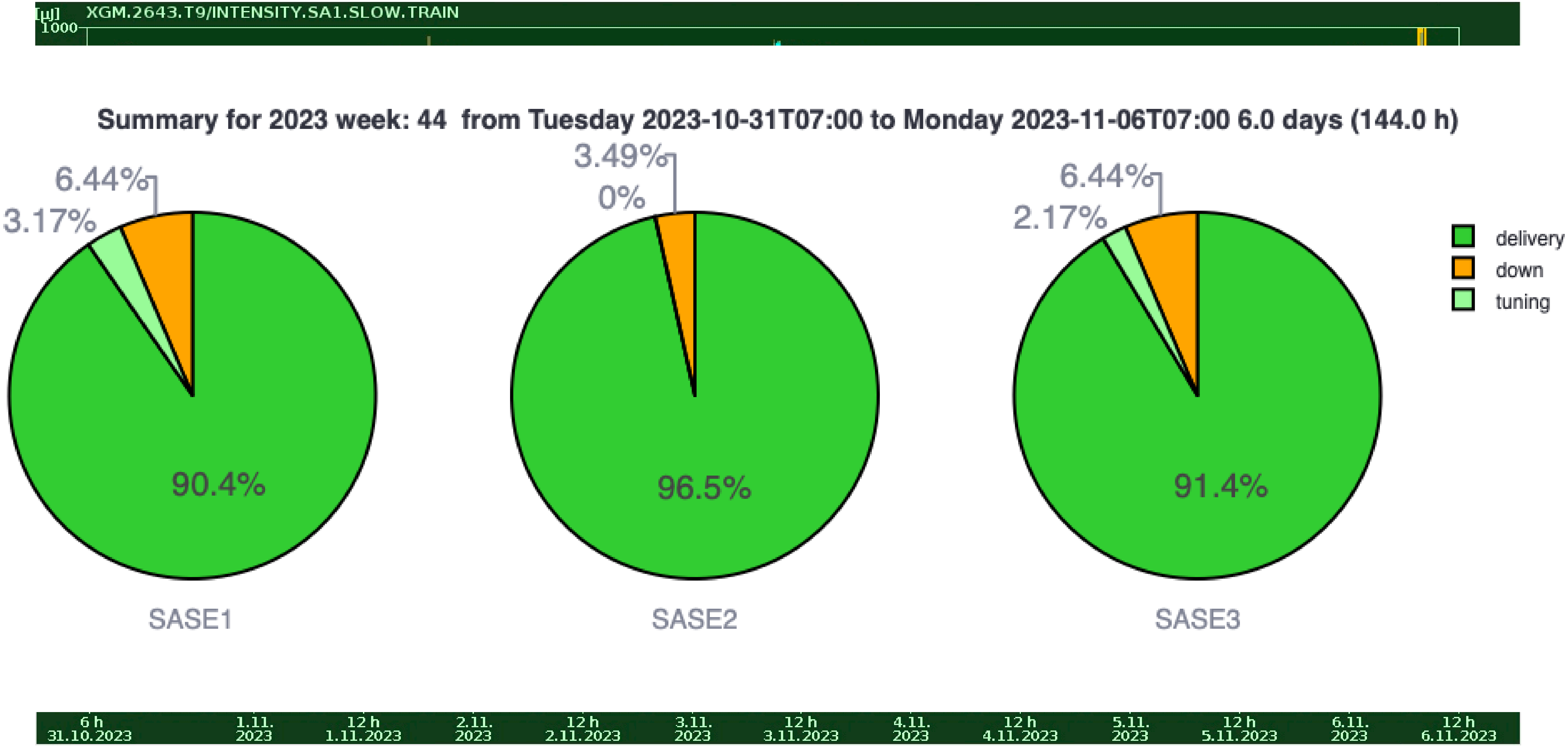

SPB / SFX

Proposal for experiment at European XFEL – Experiment description
Ultrasound-activatable droplets for brain tumor therapy

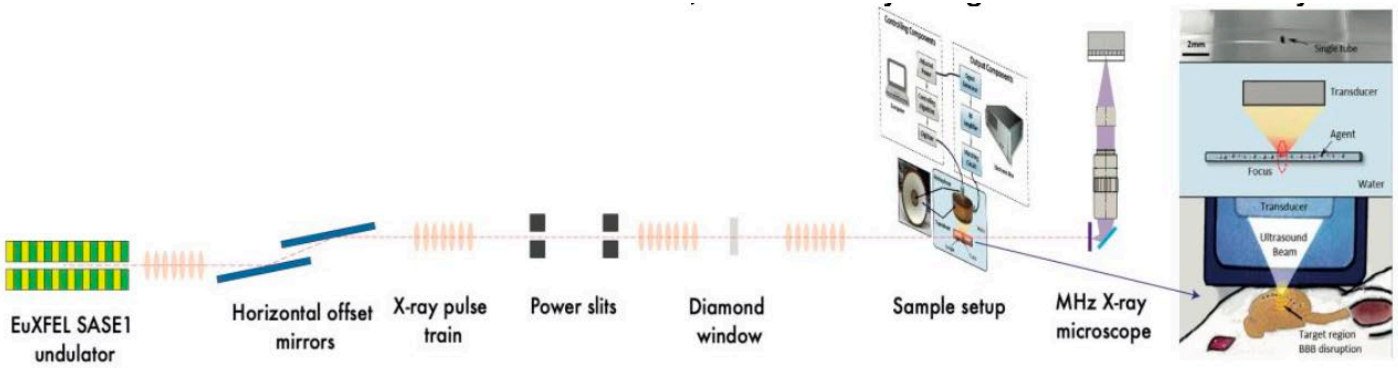

Figure 2: Experimental arrangement for the MHz X-ray microscopy of the ultrasound activated droplets

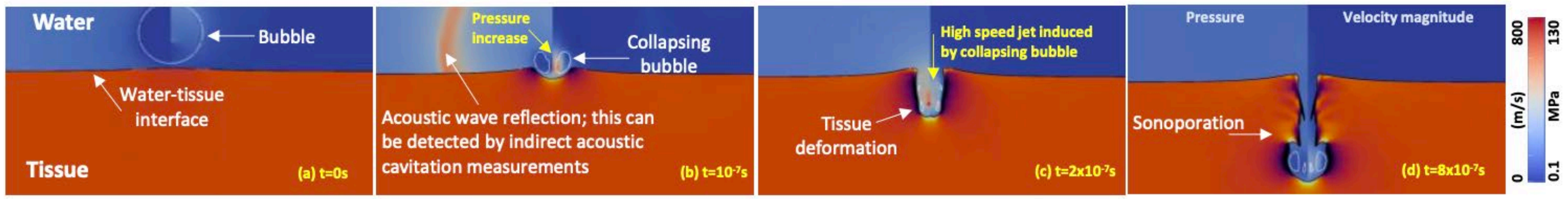

SQS

Megahertz Single-Particle Diffractive Imaging of Macromolecular Scaffolds

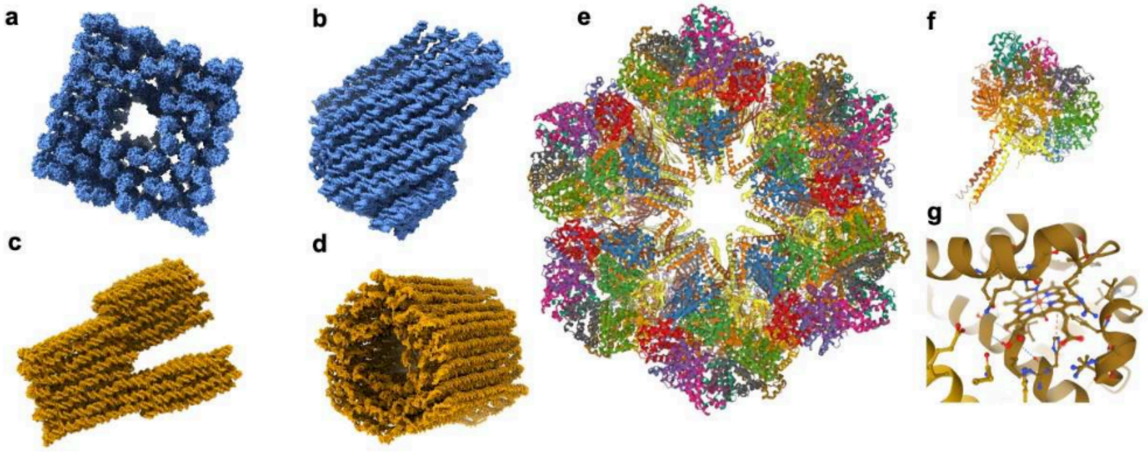

Fig 1. Cartoon representation of cryo-EM structures of a few representative 3D DNA-origami scaffolds and giant-hemeprotein erythrocruorin that we propose to image at MHz rate with DSSC at SQS. (**a**) symmetric DNA-origami cage (PDB: 6BY7) with the central cavity size of ~10nm which can be used to host small-proteins and nanoparticles; (**b**) asymmetric pointer (PDB:4V5X) with features spanning across several length scales with non-convexity. Both structures at top were run in p2322 experiment and they diffracted successfully. (**c**)Tower Twister (PDB: 7ARV), this can be used as molecular ruler. (**d**)126 helix-bundle, made through orthogonal scaffolds (~10 MDa, almost twice the size of all other three origami structures, PDB: 7AS5).[7,8] (**e**) the 3.6 MDa giant-hemeprotein erythrocruorin (PDB:2GTL), (**f**) hemoglobin dodecamer monomer subunit of erythrocruorin (**g**) CO-bound heme/porphyrin ring of erythrocruorin hemoglobin. Images are only for representation and not to scale.

MID

Proposal for experiment at European XFEL – Experiment description

Combined imaging-diffraction characterization of shock waves in metallic materials

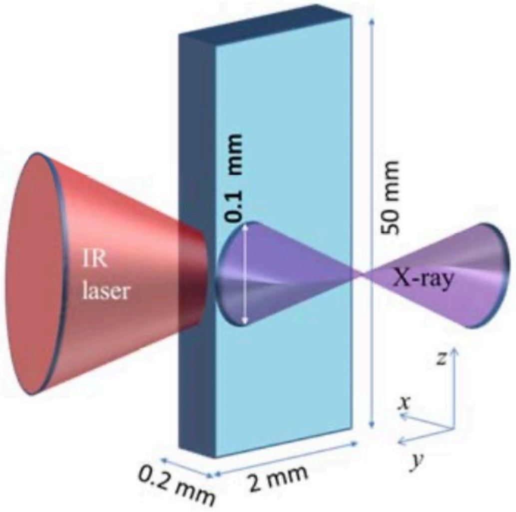

Fig. 3. Sample dimensions and schematic setup geometry of the pump and probe experiment

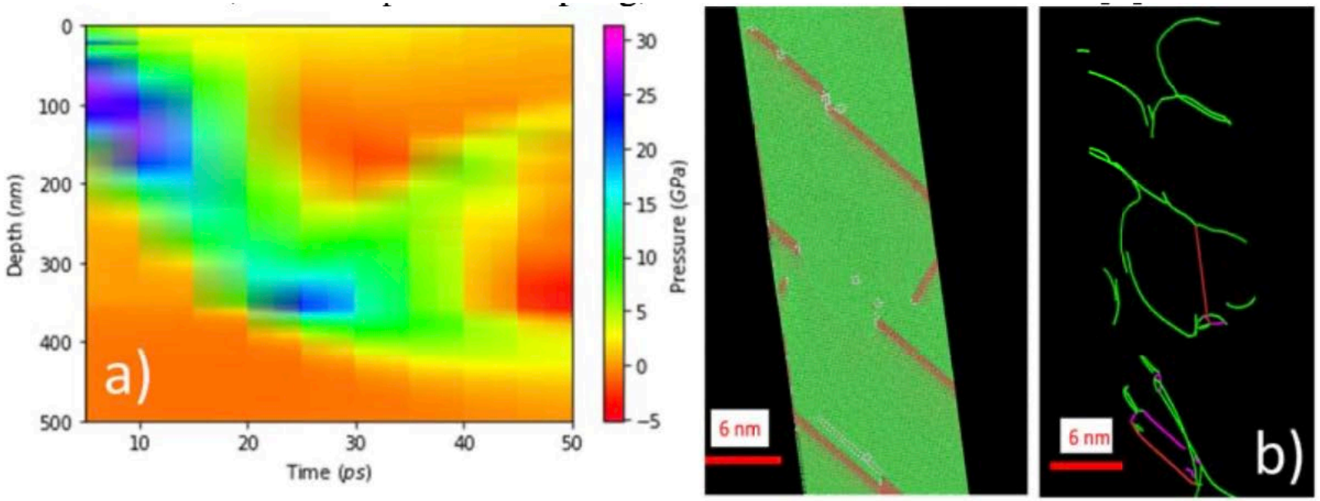

Figure 1. Pressure distribution below the surface of an Al single crystal with (001) orientation as a function of time (a) and the generation of dislocations on 111 planes below the irradiated surface by the propagating shock wave (b). (Jobs for larger models were submitted to the high performance computing center of CEA, France)

Operation Highlights in 2023 – 2025

2024

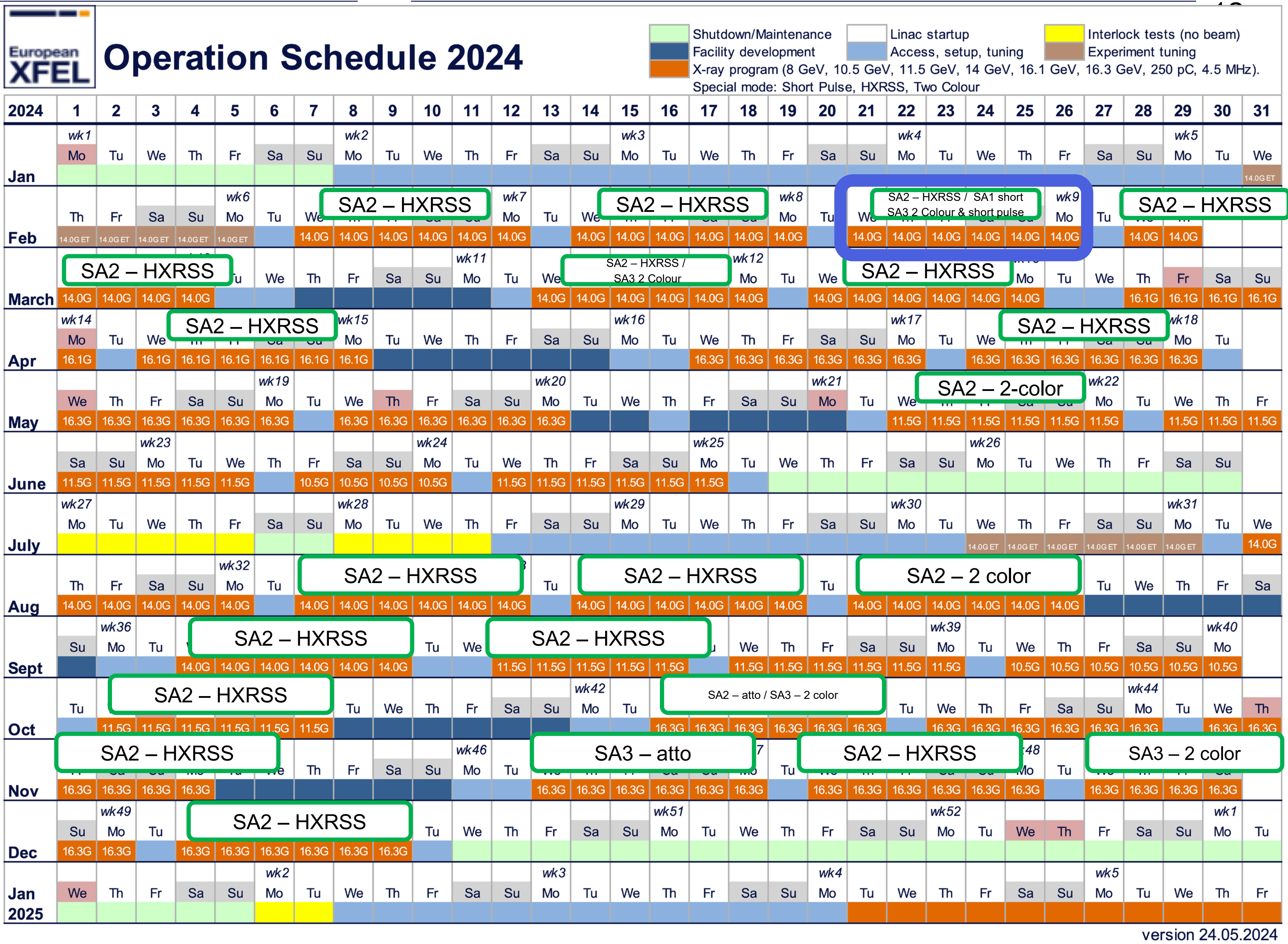

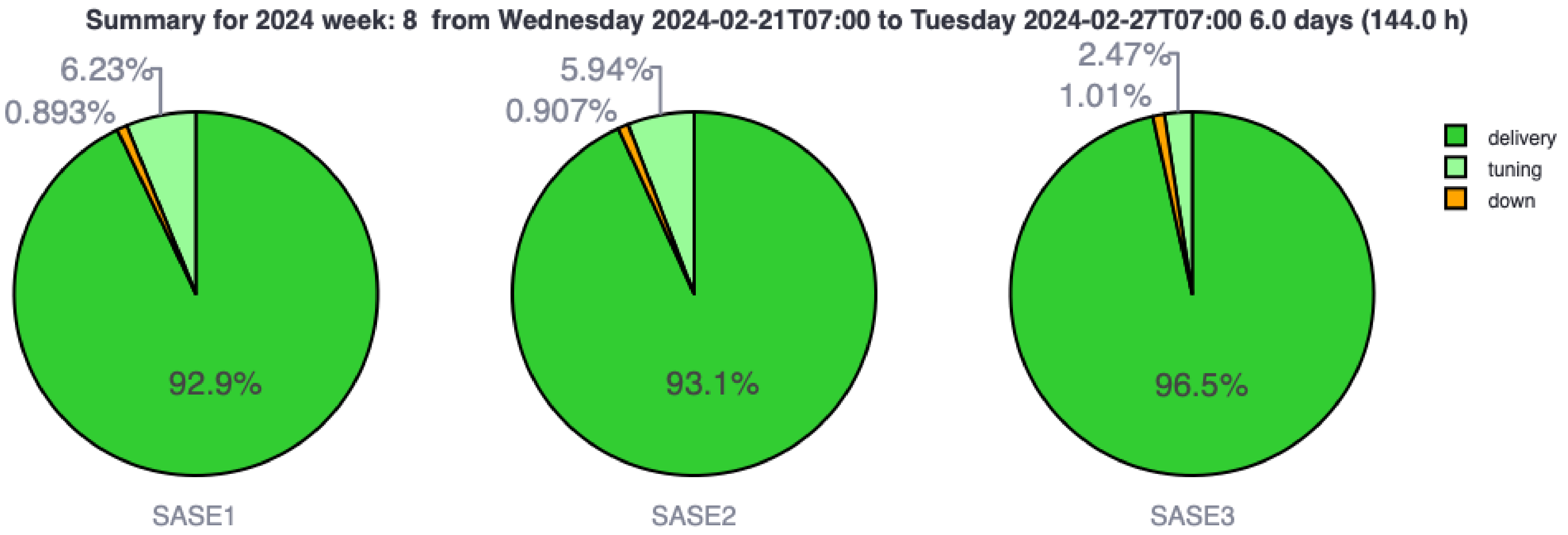

- User delivery week at 14 GeV running none standard operation modes at all three beam-lines:
  - SASE1: short pulses (aimed even for < 1 fs)
  - SASE2: HXRSS at changing wavelengths (8.5 and 10.5 keV)
  - SASE3: 2 color pump and probe
- As result all three beam-lines require very specific compression settings. In general no problem …

SPB/SFX

Single Particle Incoherent Diffractive Imaging

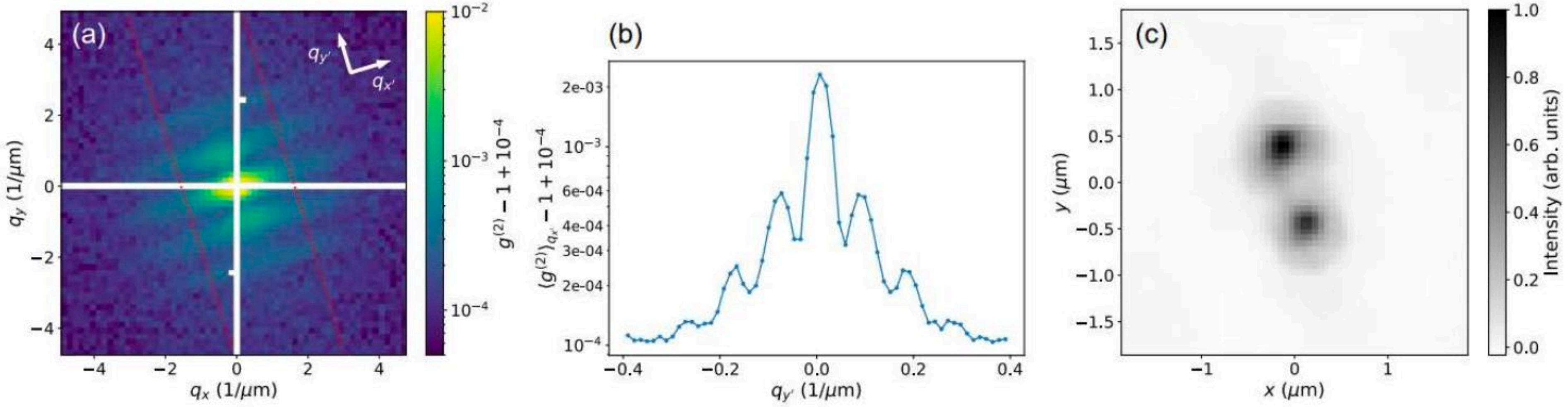

Figure 1: From Ref. [8] (a) Measured $g^{(2)}$-1 signal on a logarithmic scale. (b) 1D profile normal to fringes (shown in red in (a)). (c) *Ab initio* reconstruction of emitter distribution using iterative phase retrieval methods.

SCS

Temperature diagnostics and ultrafast ionization dynamics of XFEL-created warm dense aluminum

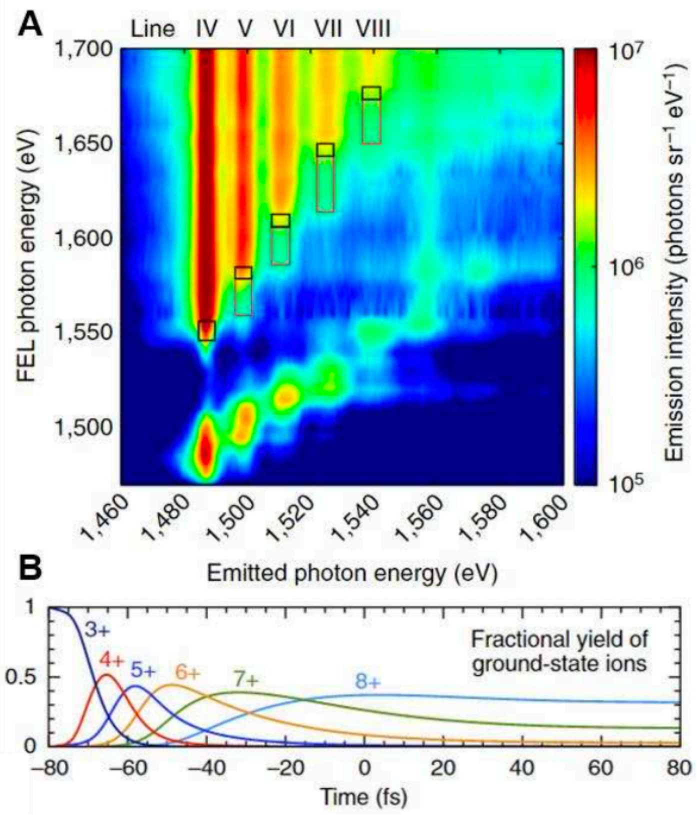

Figure 1. A) X-ray emission spectra showing the various K-alpha lines observed at LCLS [5] as a function of XFEL photon energy. We plan to study these transitions in absorption, thus accessing the time-resolved dynamics of the different ionization states of warm dense Al. B) Fractional yield of ground-state ions during irradiation of 1-µm thick Al foil by an XFEL pulse of 1630 eV central photon energy at 1x10^{17} W cm^{-2}, calculated by SCFLY, also extracted from [5]. Our proposal is to study the time-resolved intensity of the K-alpha absorption lines for a direct measure of such ionization dynamics.

HED

Generation of extreme pressure states with cylindrical imploding wires.

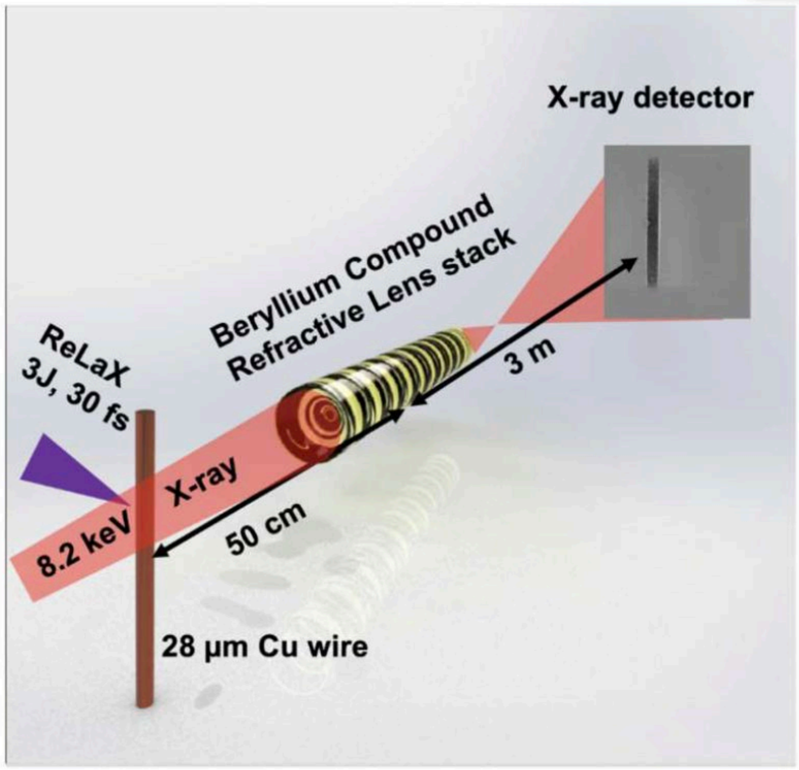

FIG. 1. Experimental setup of the imaging configuration.

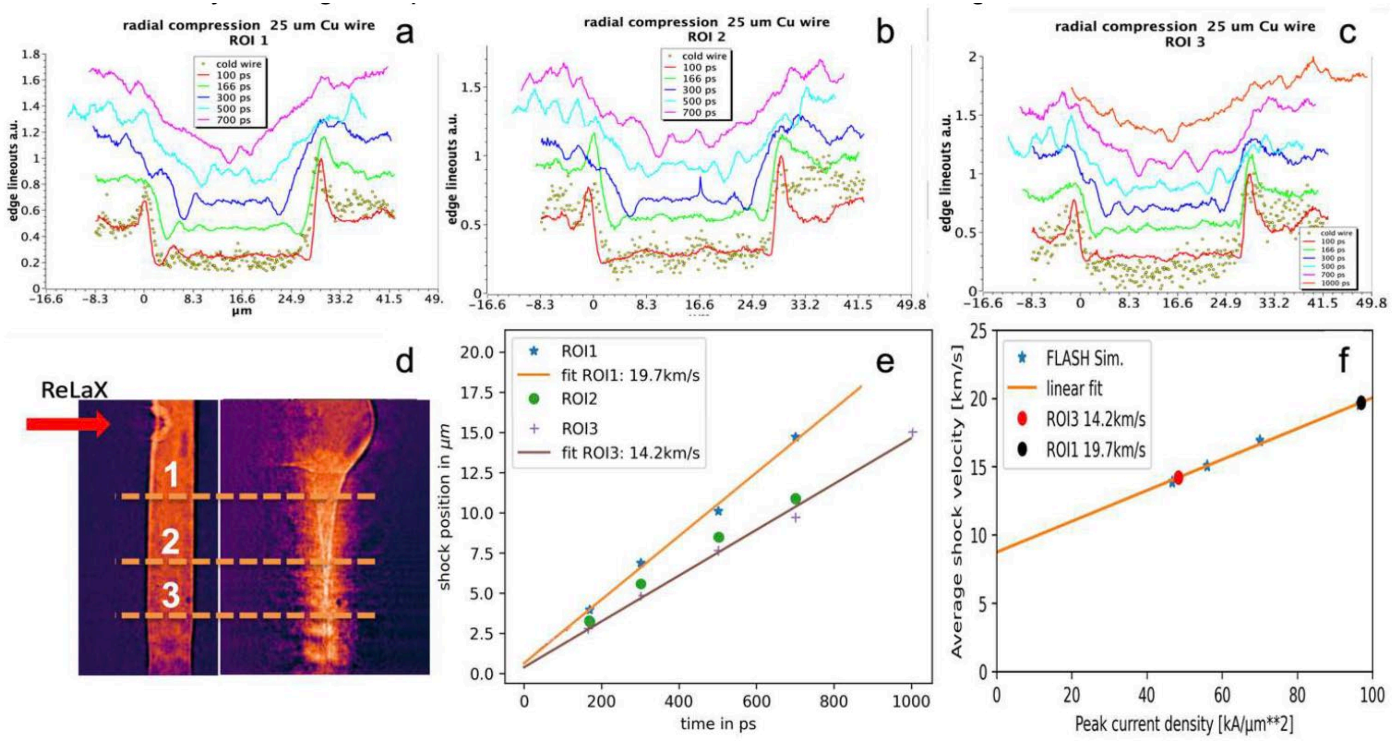

2024

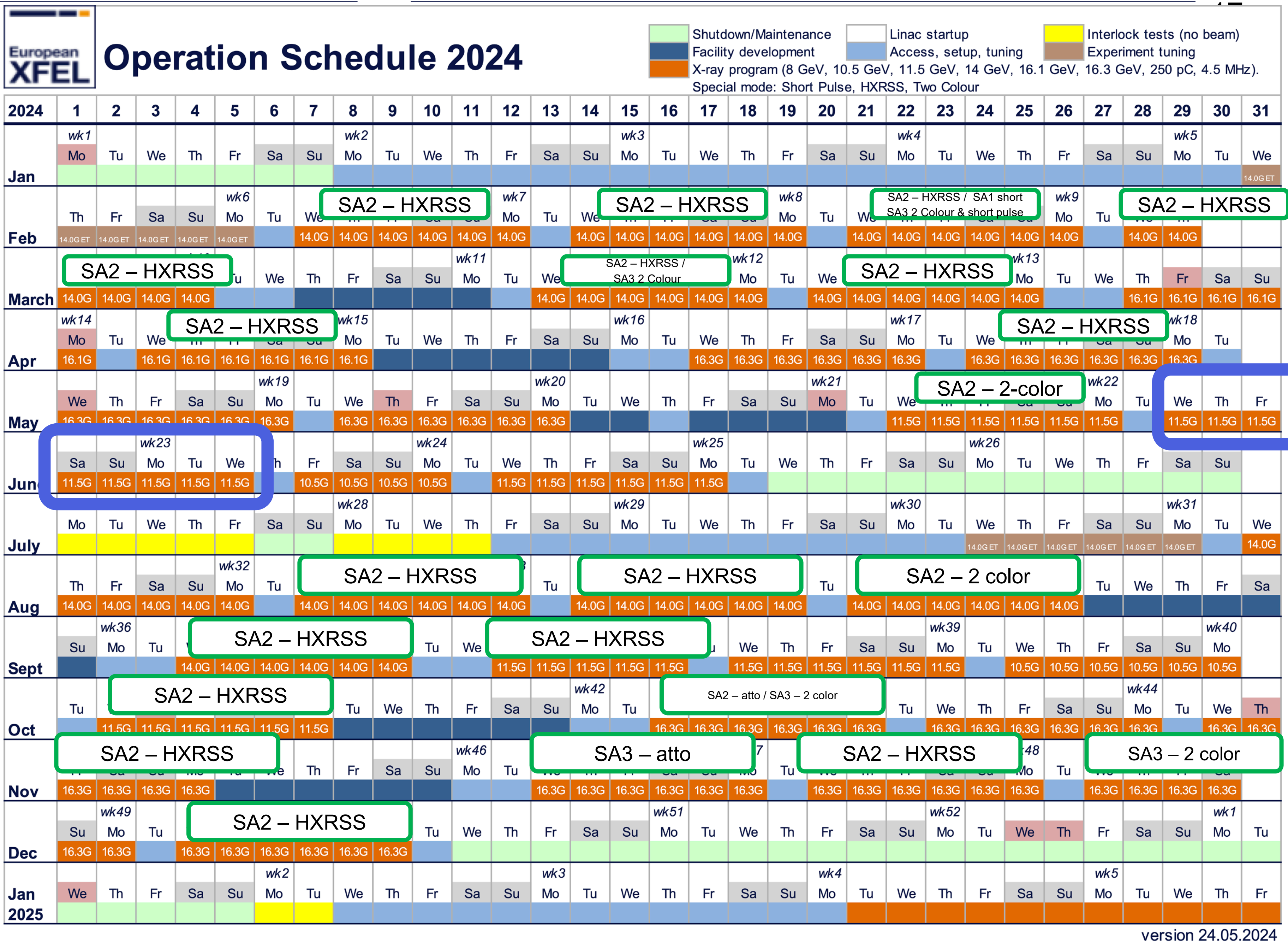
European XFEL
Operation Schedule 2024
Shutdown/Maintenance
Facility development
X-ray program (8 GeV, 10.5 GeV, 11.5 GeV, 14 GeV, 16.1 GeV, 16.3 GeV, 250 pC, 4.5 MHz).
Special mode: Short Pulse, HXRSS, Two Colour
Linac startup
Access, setup, tuning
Interlock tests (no beam)
Experiment tuning
SA2 – HXRSS
SA2 – HXRSS / SA1 short
SA3 2 Colour & short pulse
SA2 – HXRSS / SA3 2 Colour
SA2 – 2-color
SA2 – 2 color
SA2 – atto / SA3 – 2 color
SA3 – atto
SA3 – 2 color
version 24.05.2024

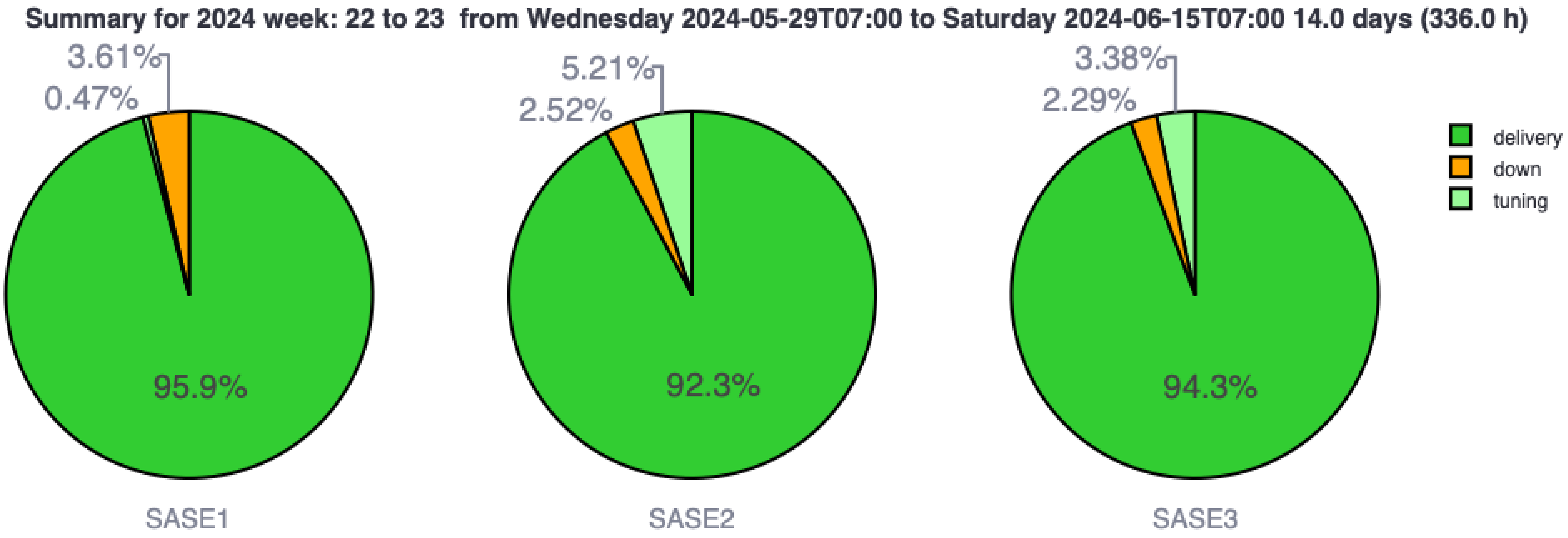
Summary for 2024 week: 22 to 23 from Wednesday 2024-05-29T07:00 to Saturday 2024-06-15T07:00 14.0 days (336.0 h)
3.61%
0.47%
95.9%
SASE1
5.21%
2.52%
92.3%
SASE2
3.38%
2.29%
94.3%
SASE3
delivery
down
tuning

MID Rolling Bunch Pattern cw 22

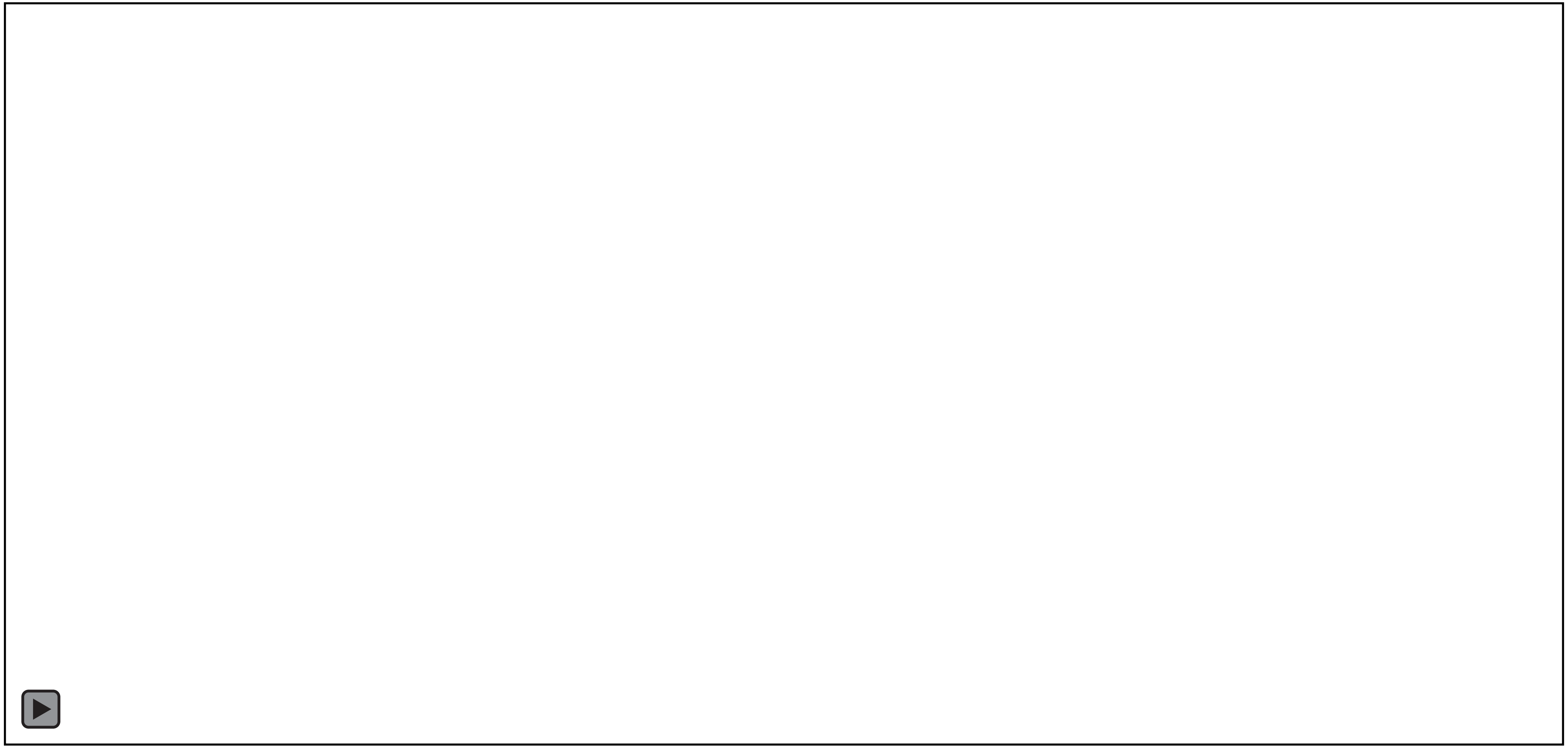

Rolling Bunch Pattern

MHz XPCS enabled studies of dynamics, interactions and aggregation phenomena in protein solutions

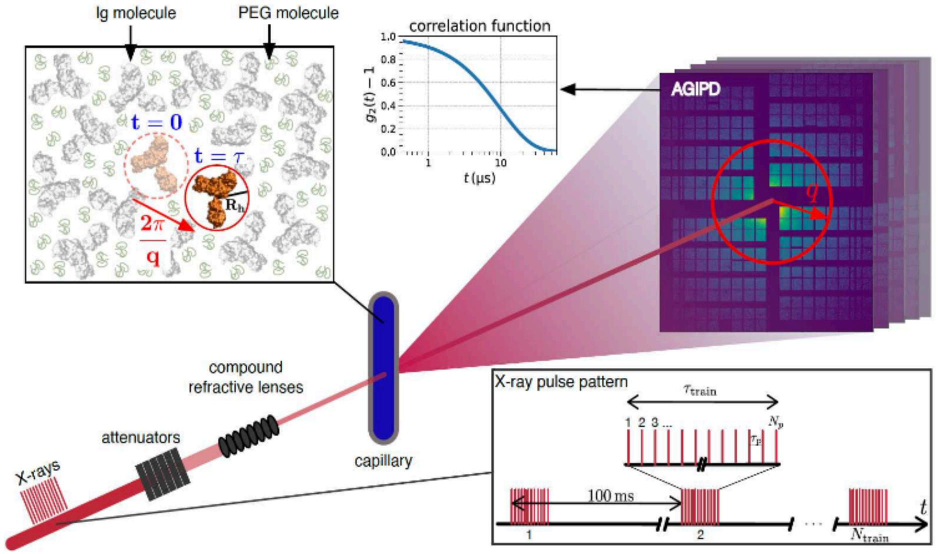

Fig. 1: Setup of MHz protein XPCS at MID used in Reiser et al. Pulses were separated by multiples of 443 or 886 ns and the capillary moved after each train to illuminate a fresh spot. The beam was attenuated using 10^8 ph/pulse (from [4]).

10^0 10^1 τ (µs) 10^0 10^1 τ (µs)

4) Experiment plan

Scheduling period	Instrument(s) requested	8-hour shifts requested	Results expected
2023/I (Jan-June 2023)	MID	8	Boost SNR, establish monochromatic XPCS
2023/II (July-Dec 2023)	MID	8	Quantify beam induced effects, identifying window for protein XPCS, ML tools and fast data analysis pipeline fully established
2024/I (Jan-June 2024)	MID	8	Quantify effects of self-crowding in D(Q) and H(Q)
2024/II (July-Dec 2024)	MID	8	Quantify effects of crowding agents, salts and osmolytes on dynamic properties
2025/I (Jan-June 2025)	MID	8	Measure dynamics during the early stages of liquid-liquid phase separation on molecular length scales
2025/II (July-Dec 2025)	MID	8	Dynamics of denaturation and aggregation processes via IR Pump – MHz probe XPCS

FXE – cw 22

Capturing dynamics of polaron formation in hematite by x-ray absorption spectroscopy

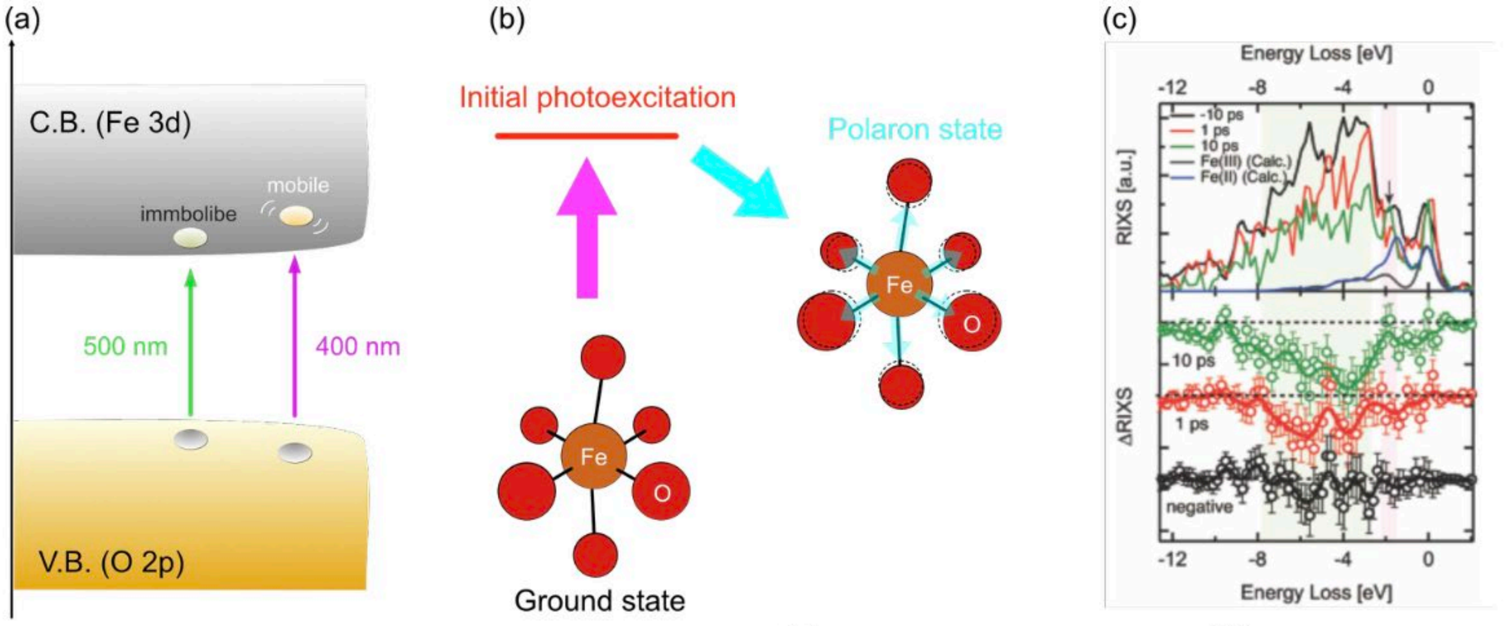

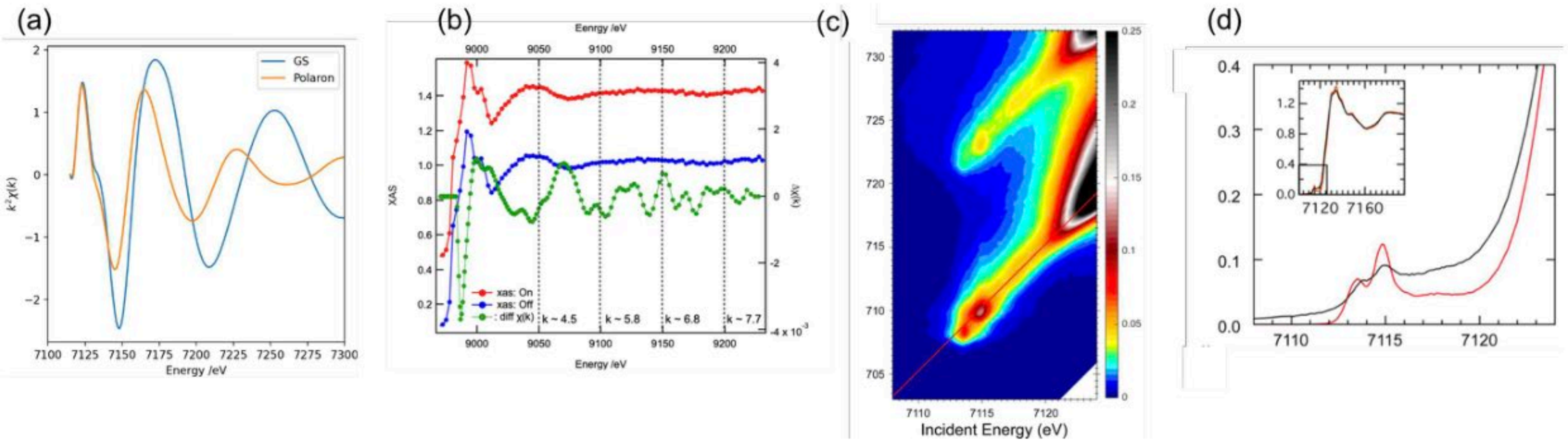

SCS

Proposal for experiment at European XFEL – Experiment description Enabling synthetic control of intersystem crossing dynamics in photoluminescent chromium complexes

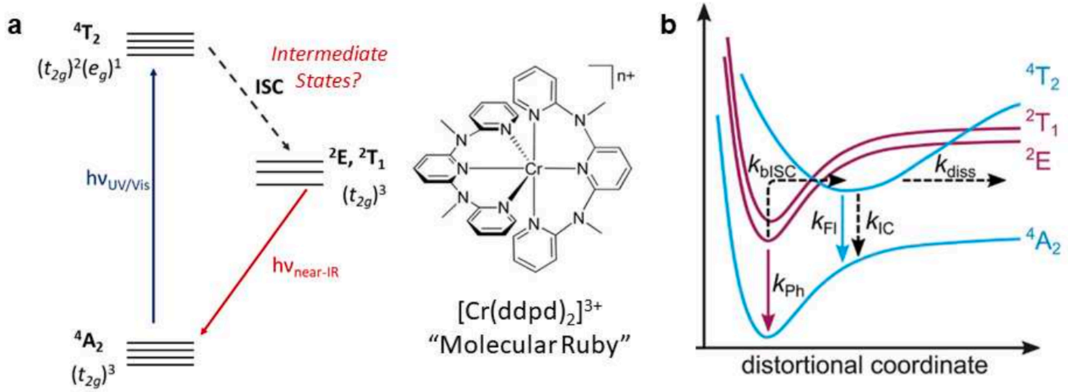

Figure 1. **a** Diagram of photochemical cycle for spin-flip emission together with structure of $[Cr(ddpd)_2]^{3+}$. **b** Numerous non-radiative processes (dashed black lines) contribute to deactivation of spin-flip emission (k_{Ph}) including back bISC (k_{bISC}), internal conversion (k_{IC}), molecular dissociation (k_{diss}).

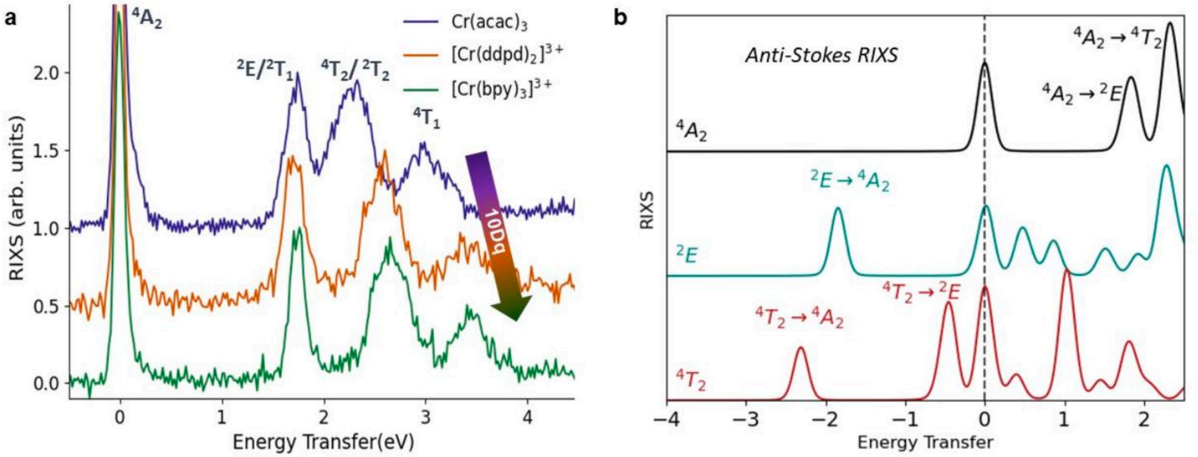

Figure 2. **a** Static RIXS spectra of Cr^{3+} complexes measured on powder samples. **b** RIXS spectra of ground and lowest lying excited states calculated using ligand field multiplet theory with parameters corresponding to $Cr(acac)_3$. The incident energy was set to Cr L_3-pre-edge region in the simulations.

SQS

Dynamics of electron solvation in aqueous systems

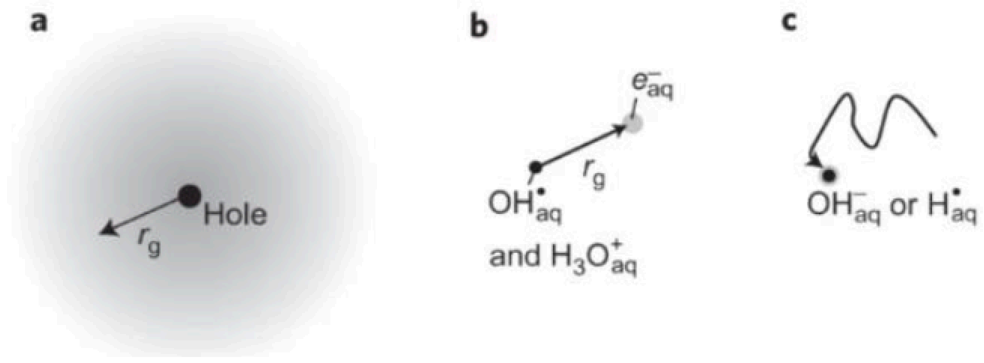

Figure 1 ***a****. Ejected delocalized excess electron (in grey) with radius r_g.* ***b****. Collapse of the electron wavefunction, which will result in an average ejection length r_g.* ***c****. Diffusive geminate recombination. From Ref. [17]*

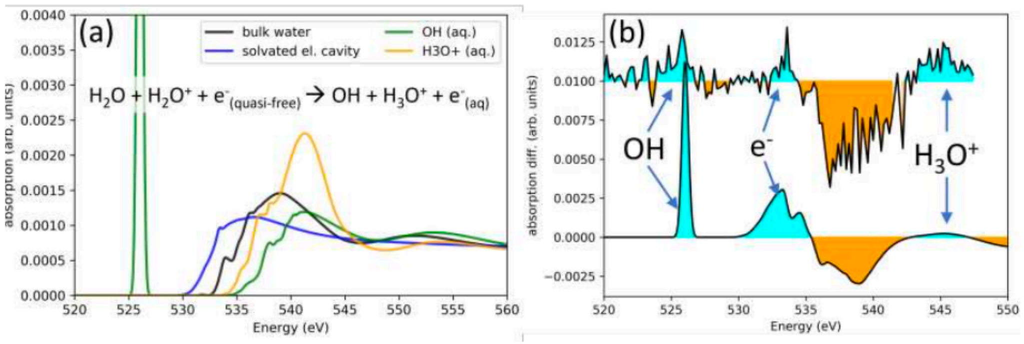

Figure 3. X-ray absorption spectra of the species generated following ionization of liquid water. (a) Calculated XAS for bare water, OH radical, H_3O^+, e^-_{aq} in water. (b) Experimental (top) and calculated (bottom) difference XAS for water containing OH radical, H_3O^+, and a solvated electron cavity. The calculated XAS differences are constructed by subtracting the spectrum of the ion, radical, or cavity molecule from the one of bare liquid water using the same sampling methodology, respectively. Because a cavity is constructed by 4–5 water molecules, the cavity-difference signal is weighted by a factor of 4.5 compared to the difference signal of the hydronium cation and the hydroxyl radical.

2025

Summa

h)

SA1
1.0
0.31

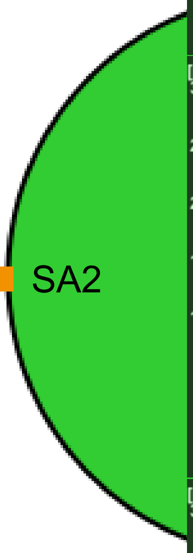

SA2

SA3

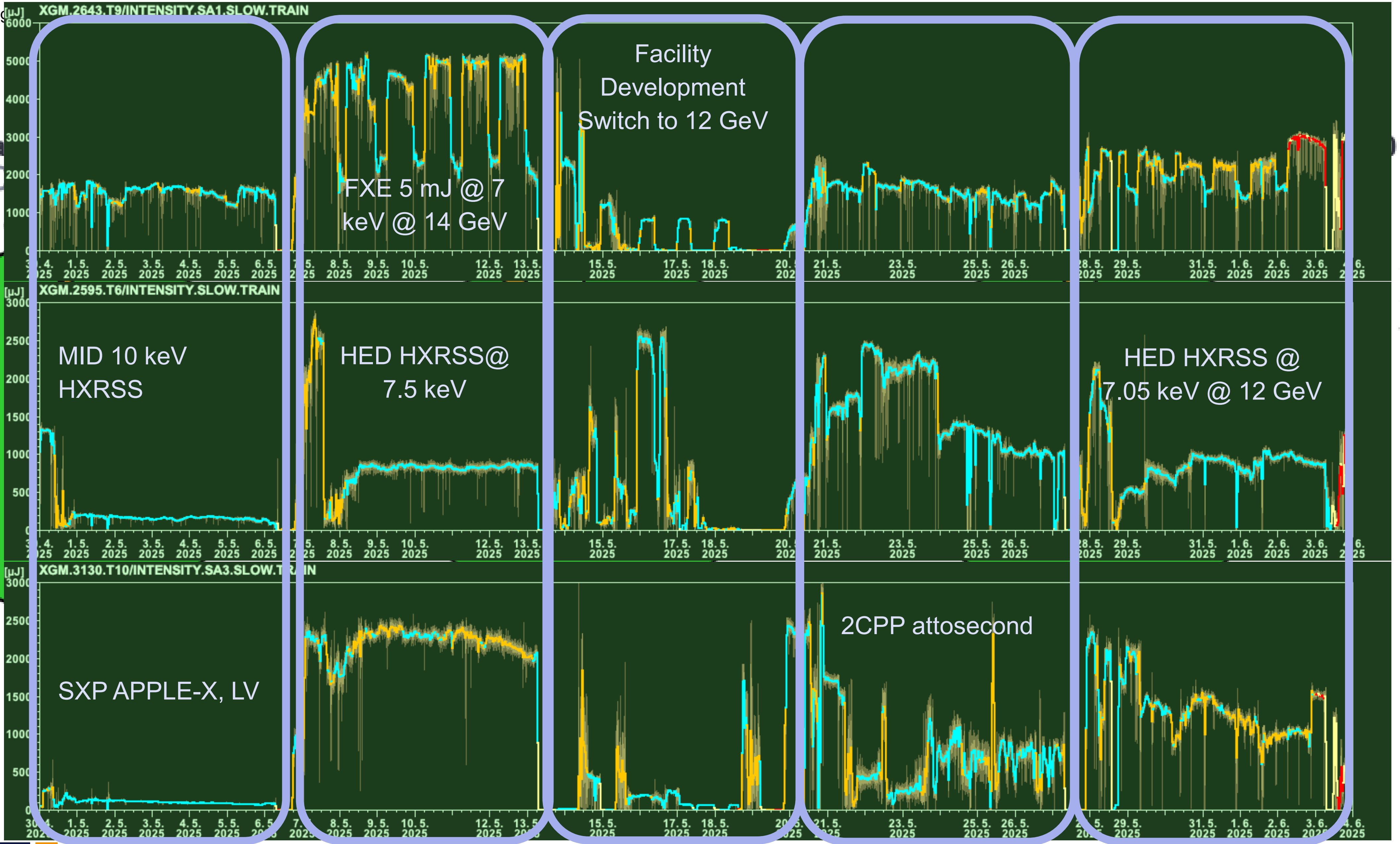

delivery
down
tuning

Machine Statistics (cw 23)

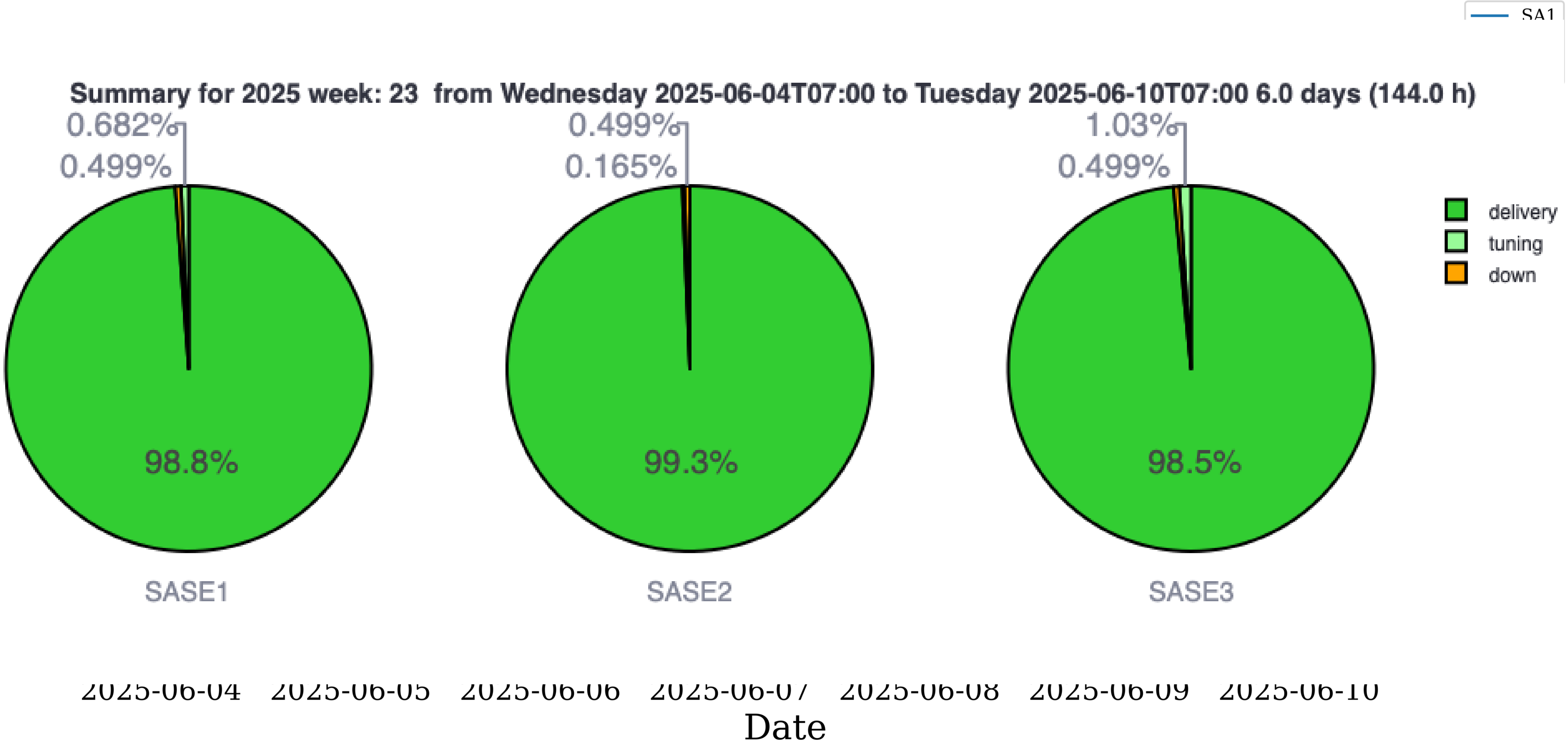

100 W average @ SA3, 700 eV

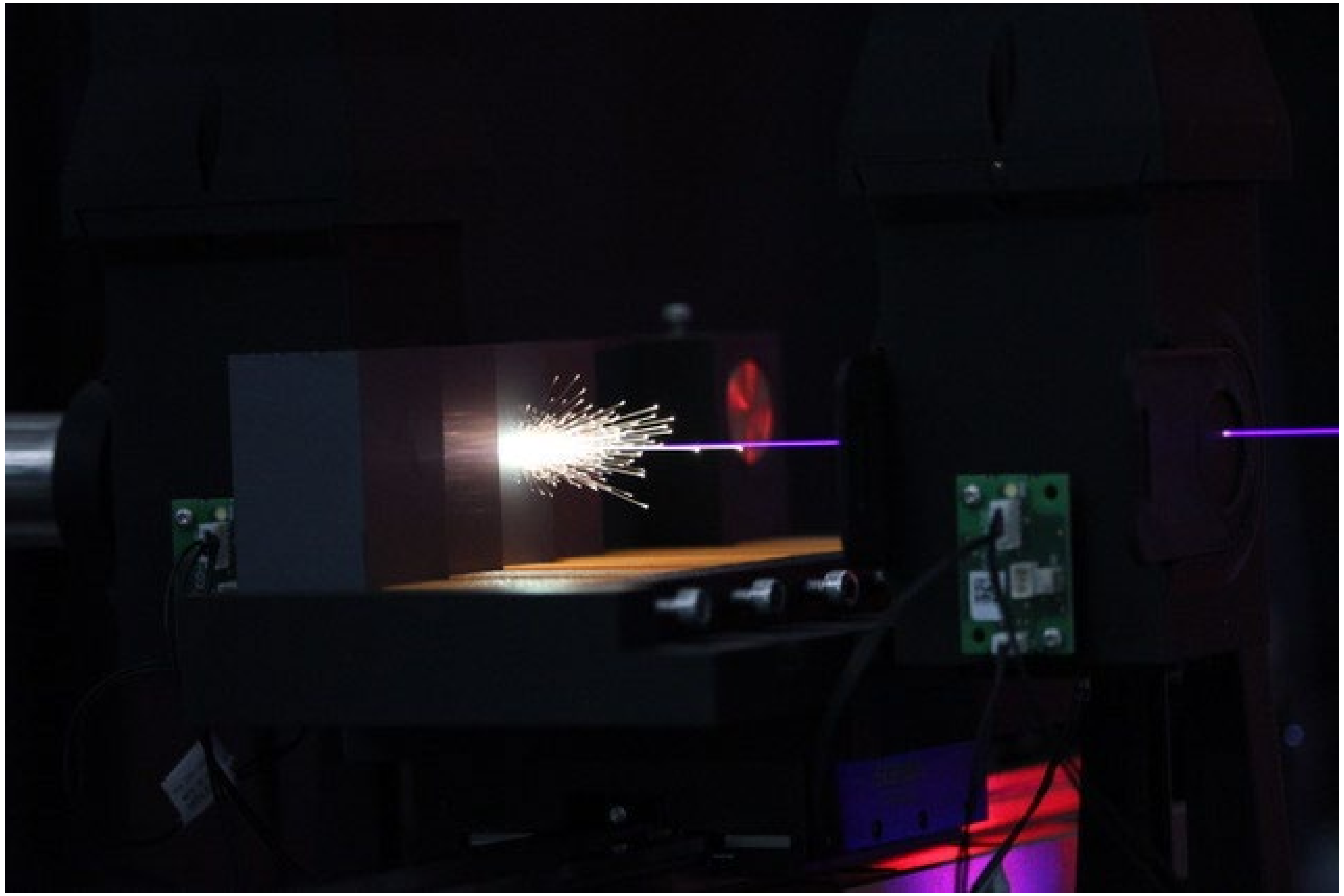

Example:
2024 annual schedule showing *non-standard delivery modes*

- Non-standard delivery modes
  - HXRSS@SA2
    - ► 16/32 wks = 50%
  - Ultrashort pulses (attoscnd)
    - ► 1 wk SA3
    - ► 1 wk SA2
  - Other
    - ► 2-color
    - ► Variable polarization

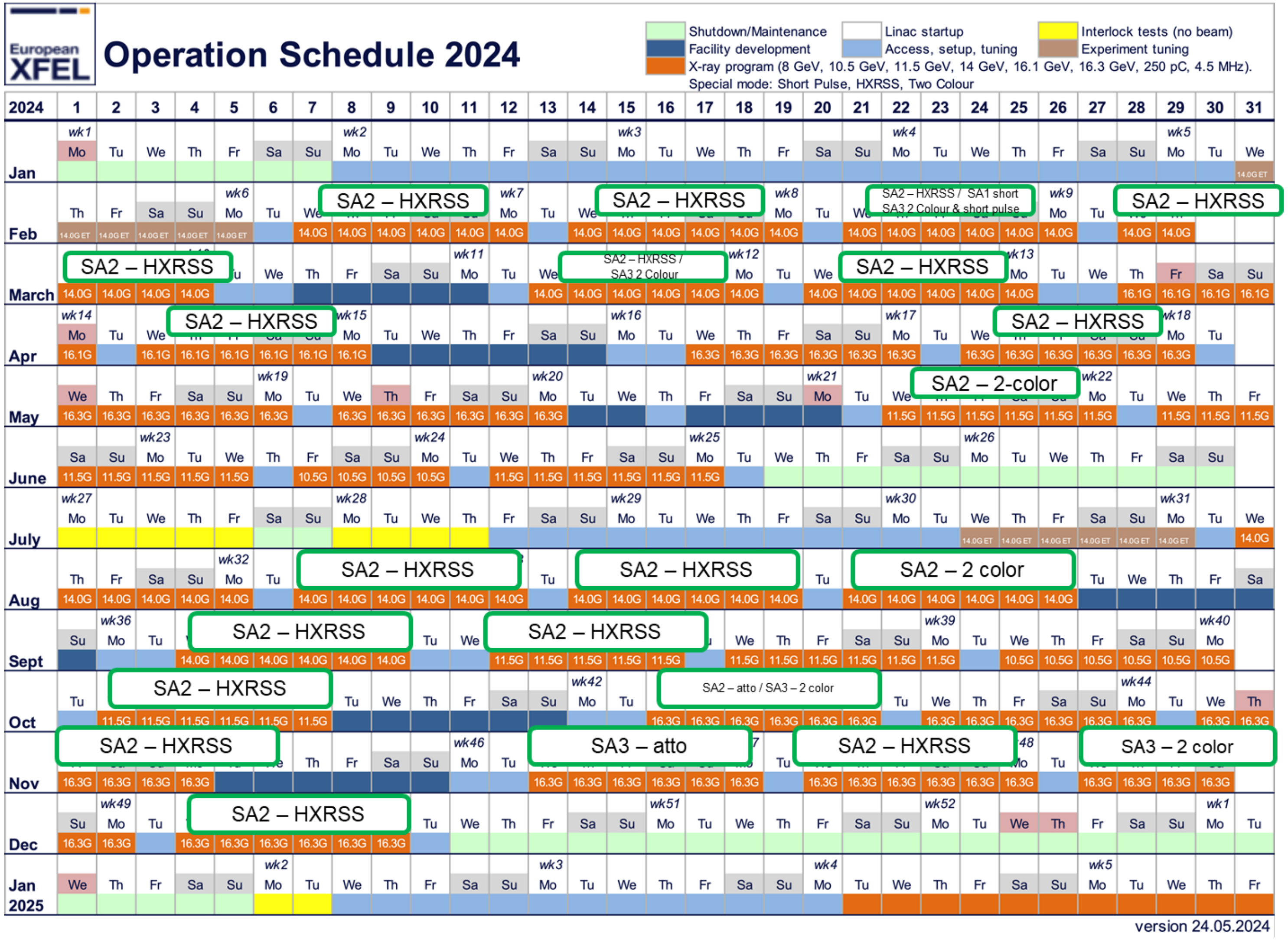

Scheduling non-standard modes 2023 to 2025

2023:

- SA3 2-color: 3
- SA3 short-pulse: 1
- SA3 short-pulse + 2-color: 1
- SA2 2-color: 1
- SA2 HXRSS: 9
- **Total: 15 wks**

2024:

- SA3 2-color: 3
- SA3 short pulse: 0
- SA3 short pulse + 2-color: 1
- SA3 atto: 1
- SA2 2-color: 2
- SA2 HXRSS: 17
- SA2 atto: 1
- **Total: 25 wks**

2025 (only 1st half)

- SA3 2-color: 0
- SA3 short-pulse: 0
- SA3 atto + 2-color: 1
- SA3 atto: 1
- SA3 circular: 1
- SA2 HXRSS: 7
- SA2 atto: 1
- **Total: 11 wks**

Resonant excitation of the nuclear clock isomer ^{45}Sc

- Resonant oscillators with stable frequencies and large quality factors determine our ability to keep track of time with high precision
- Nuclear oscillators surpass their atomic counterparts by their naturally higher quality factors and higher resilience against external perturbations
- The 12.4 keV nuclear transition in ^{45}Sc
  - Ultranarrow transition linewidth: 1.4 femto-eV
  - Extreme metrology and ultraprecise frequency standards

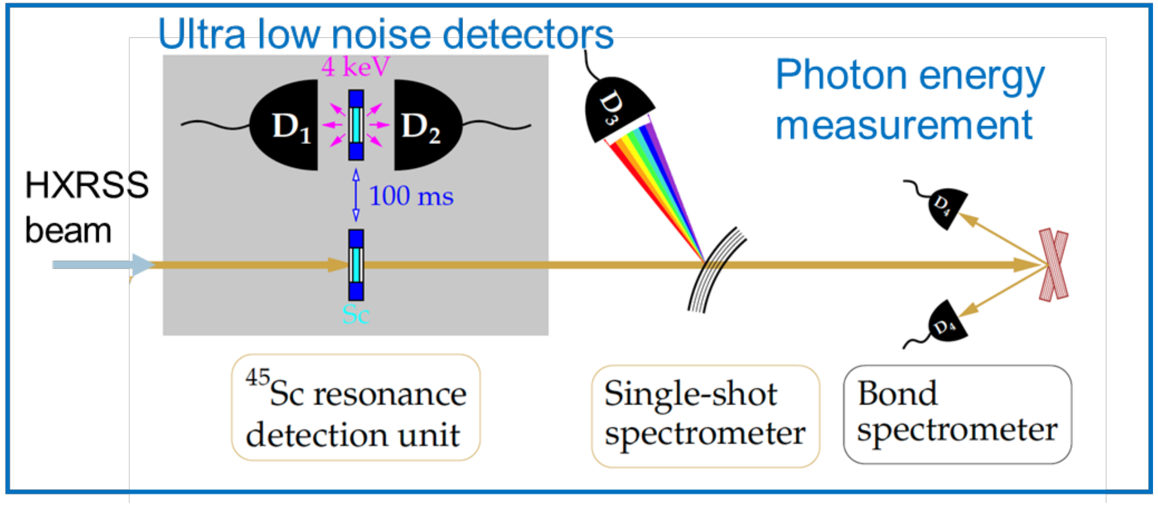

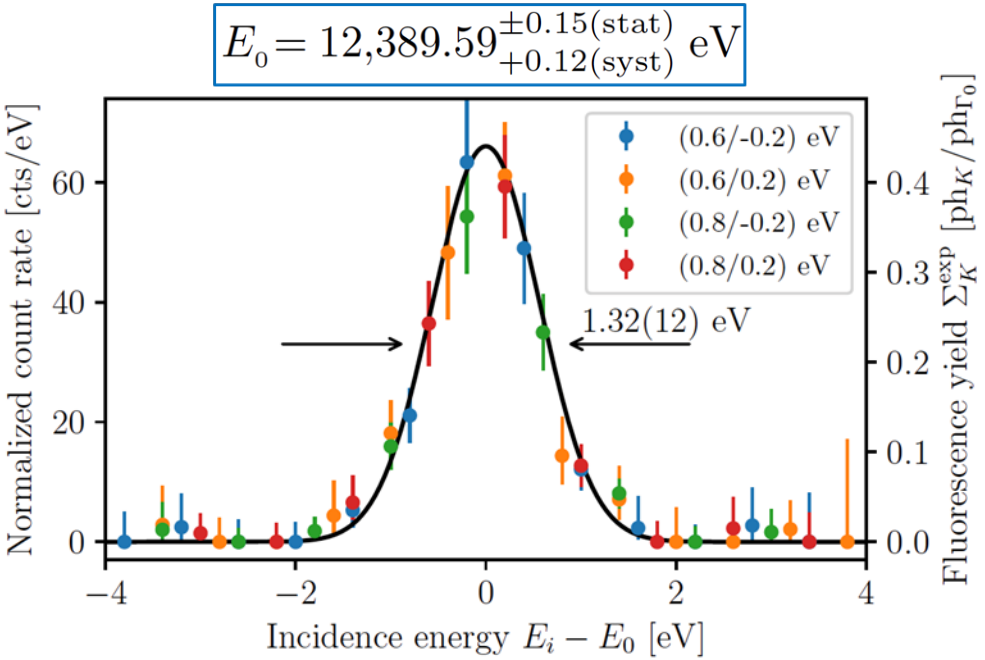

Yu. Shvydko *et al.*, Nature 622 (2023)

Thank you
for your attention